

Thermomagnetic effect in oxygen interacting with gold and platinum surfaces

V. D. Borman, S. Yu. Krylov, B. I. Nikolaev, V. A. Ryabov, and V. I. Troyan

Moscow Engineering Physics Institute

(Submitted April 5, 1976)

Zh. Eksp. Teor. Fiz. 71, 1373-1389 (October 1976)

Results are presented of an experimental and theoretical study of the thermomagnetic effect (TME) in oxygen interacting with gold and platinum surfaces. The effect consists of a change in the heat flux through very low pressure gas in the gap between two surfaces at different temperatures when a magnetic field is established in the gap. The effect is due to the nonspherical nature of the interaction between the molecules and the surface of a solid. TME in oxygen is found to depend on the material of the surface. It is also found that, in contrast to previously studied nonparamagnetic gases (N_2 , CO, CO_2) interacting with a gold surface, the TME anisotropy (dependence of the magnitude of the effect on field direction) is anomalous in the case of O_2 . A theory of TME is developed for a gas whose molecules have nonzero resultant electron spin. Comparison of this theory with experimental data is used to determine the explicit form of the nonspherical part of the scattering amplitude for O_2 on Au and Pt. Comparison of experimental and theoretical results has also led to the conclusion that the O_2 molecules leaving Au and Pt surfaces are predominantly in states in which the component of the electron spin along the total angular momentum is zero.

PACS numbers: 79.20.Rb

1. INTRODUCTION

The thermomagnetic effect (TME) in a highly rarefied gas was predicted and discovered in^[1,2]. It involves a change in the thermal flux Q through a molecular gas in the gap between two surfaces at different temperatures when a magnetic field H is introduced into the gap. It occurs when the mean free path λ of the molecules is much greater than the separation L between the surfaces. It is shown in^[1,3,4] that TME is due to the nonspherical nature of the interaction between the molecules and the solid surfaces. The net effect of this interaction is that the gas molecules become polarized, and the precession of these molecules in the magnetic field produces partial removal of this polarization, i. e., averaging of the angular momenta of the molecules in the plane perpendicular to the magnetic field. When the energy transfer during the interaction with the surface depends on the orientation of the molecule, the change in the polarization should lead to a change ΔQ in the heat flux. Hence, it is clear that the parameter which determines ΔQ is the product $\omega\tau$, where $\omega \sim \mu H$ is the frequency of precession of the molecules, μ is the magnetic moment, $\tau = L/v$ is the time spent between walls, and v is the mean velocity. In addition, the quantity ΔQ should depend on the direction of the field. It is also shown in^[1,3,4] that the dependence of ΔQ on $\omega\tau$ should have the form of a damped oscillation. These predictions have been established experimentally for N_2 , CO, and CO_2 interacting with Au surfaces in^[5]. This paper also gave a theory of TME which described the experimental data and could be used to solve the converse problem, namely, the problem of comparing experimental data with theoretical predictions in order to establish an expression for the nonspherical part of the probability of scattering of molecules by the surface.

In this paper, we report the results of an investigation

of TME in oxygen interacting with gold and platinum surfaces. In the ground state, the O_2 molecules have an uncompensated resultant electron spin $s=1$. The magnetic fields that are necessary for the observation of the effects ($\omega\tau \sim 1$) are therefore lower by three orders of magnitude as compared with the case of nonparamagnetic gases. The apparatus used to investigate TME in paramagnetic gases, the heat-sensitive detectors, and the experimental procedure are all described in Sec. 2.

The experiments described in Sec. 3 have shown, in particular, that the quantity $\Delta Q_{\text{sat}}^{\parallel} / \Delta Q_{\text{sat}}^{\perp}$ (ratio of the values of ΔQ when the magnetic field is, respectively, parallel and perpendicular to the normal to the surface as $H \rightarrow \infty$) is anomalously low in oxygen (in contrast to N_2 , CO, and CO_2) and depends on the material of the surface. The functions $\Delta Q(H)$ for O_2 are nonmonotonic, just as in the case of N_2 , CO, and CO_2 .^[5] In oxygen, this function has two maxima which are identified with contributions of O_2 molecules in states in which the component σ of the electron spin along the total angular momentum is ± 1 or 0.

The theory of TME in oxygen is developed in Sec. 4. TME in O_2 had to be considered separately because it was necessary to take into account the possible dependence of the probability of scattering by the surface on the spin of the molecule.

Comparison between theory and experiment, given in Sec. 5, is used to determine expressions for the nonspherical part of the probability of scattering of O_2 molecules by Au and Pt surfaces. Analysis of these expressions has shown that the most probable orientations of the O_2 molecules leaving the Au and Pt surfaces are orientations with the axis parallel to the surface. It is also found that O_2 molecules leaving the Au and Pt surfaces are predominantly in states with $\sigma=0$.

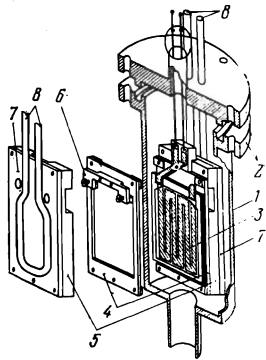


FIG. 1. Design of the probe.

2. APPARATUS AND METHOD OF MEASUREMENT

TME in oxygen interacting with gold or platinum surfaces was investigated with apparatus similar to that used previously in^[5,6].

In measurements of the heat flux in magnetic fields respectively perpendicular and parallel to the normal to the solid surface, we used Helmholtz coils and a solenoid producing a magnetic field perpendicular to the field produced by the Helmholtz coils. The latter field was arranged so that it was parallel to the earth's magnetic field H_E . This was necessary because the earth's magnetic field is of the same order (approximately 0.05 Oe) as the fields used for investigating TME in oxygen. It is therefore necessary either to correct the experimental results for the effect of the earth's field or to arrange for a complete compensation of the earth's field, and this is, in fact, achieved in the above parallel arrangement (see^[6]). The design of the probe used in these experiments is illustrated in Fig. 1. The probe consists of a cylindrical brass chamber 1, 60 mm in diameter and 160 mm long, containing the heat-sensitive element 3 carried by a top plate centered on the flanges 2. The heat-sensitive element is similar in design to that used previously in^[5] and is in the form of a 5- μ mica plate (46 \times 60 mm) held between two mica frames, 20 μ thick, to ensure sufficient rigidity. Each side of the mica plate is coated with a thin metal deposit (gold or platinum) used as a resistance thermometer. The heat-sensitive element acts as the "hot" surface and is placed between two brass frames 4 which produce a gap of 1.6 mm between the element and the "cold" surface 5. The heat sensitive element is held between the brass frames by the clamp 6. This design prevents the deformation of the heat-sensitive element when it is heated by an electric current. The cold surface is in the form of polished brass plates coated with gold or platinum, depending on the thermistor material. The entire assembly (heat-sensitive element and cold surfaces) is fixed between copper plates 7 provided with U-shaped copper tubes 8 used for cooling and thermostating the cold surfaces.

The vacuum system could be used to produce pressures of less than or approximately equal to 10^{-5} Torr in the probe. Gas release from the probe walls was $\leq 5 \times 10^{-5}$ Torr/h. The minimum working pressure ($\sim 10^{-3}$ Torr) under the experimental conditions corresponded to a Knudsen number (Kn) in oxygen of ~ 30 .

The method used to investigate the TME was similar to that described in^[2,7]. The absolute relative change in the heat flux in the magnetic field ($\Delta Q/Q$) was determined by comparing measurements performed in a broad range of pressures ($0.08 \leq Kn \leq 20$) with the data reported in^[8] for the Senteleben effect in oxygen (i. e., for $\Delta Q/Q$ in the case where $Kn \ll 1$). The calibration error in the measured values of $\Delta Q/Q$ did not exceed 10%.

Subsequent comparison of the experimental results with theoretical predictions (see Secs. 4 and 5) require a knowledge of the diffuse reflection coefficient α for O_2 molecules on Au and Pt. The coefficient α was calculated from measurements of the heat flux Q_0 (in the absence of the field) for free-molecular heat transfer between two gold or platinum surfaces, one of which was held at $T_1 = 120^\circ C$ and the other at $T_2 = 25^\circ C$.

The expression for the heat flux Q_0 (in the absence of the field) under free-molecular conditions is obtained in Sec. 4 [see (4.16)]. Equation (4.16) can be used to determine the relation between the diffuse reflection coefficient α and the measured quantities Q_0 , T_1 , T_2 , S and p (S is the area of the hot surface):

$$\alpha = \frac{2Q_0}{p} \left[\frac{Q_0}{p} + \frac{3}{2} \sqrt{\frac{2k}{\pi m}} (\sqrt{T_1} - \sqrt{T_2}) S \right]^{-1}. \quad (2.1)$$

Measurements for $Kn \geq 8$ show that the heat flux decreases linearly with decreasing pressure (for $Q_0/p = \text{const}$). This suggests that heat transfer occurs as a result of collisions between the O_2 molecules and the surface. The diffuse reflection coefficient for O_2 on Au and Pt, calculated from (2.1), is found to be 0.85 ± 0.03 and 0.92 ± 0.03 , respectively.

3. TME MEASUREMENTS ON OXYGEN INTERACTING WITH GOLD AND PLATINUM SURFACES

Figures 2 and 3 show the measured relative change in the heat flux ($\Delta Q/Q$) in oxygen between platinum (Fig. 2) and gold (Fig. 3) surfaces, one of which was held at $120^\circ C$ and the other at $25^\circ C$, as a function of the magnetic field in a broad range of pressures ($p = 0.390 - 0.0016$ Torr) with the magnetic field H perpendicular (Figs. 2a and 3a) and parallel (Figs. 2b and 3b) to the normal k to the solid surfaces, respectively.

It is clear from these figures that, for pressures $p \geq 0.008$ Torr ($Kn \leq 4$), the ratios $(\Delta Q/Q)^{\perp}$ and $(\Delta Q/Q)^{\parallel}$ decrease monotonically with increasing H down to $(\Delta Q/Q)_{\text{sat}}^{\perp}$ and $(\Delta Q/Q)_{\text{sat}}^{\parallel}$, respectively. This dependence of $\Delta Q/Q$ on H is connected with the change in the heat-transfer coefficient κ of oxygen in the magnetic field (Senteleben effect; see, for example, ^[8,9]). It is clear that, as the pressure decreases, this effect should vanish because its main cause, i. e., collision of nonspherical molecules, is then removed.

For pressures $p \leq 0.004$ Torr, when $Kn \geq 8$ and heat transfer between the two surfaces held at different temperatures is largely due to collisions between the molecules and the surfaces, the function $\Delta Q(H)$ exhibits the characteristic maxima predicted by the theory for highly rarefied gas.^[1,3,4]

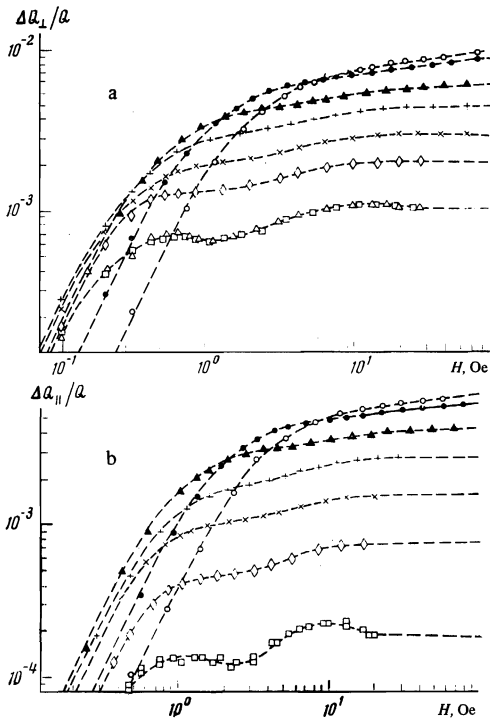


FIG. 2. Ratio $\Delta Q/Q$ as a function of H for O_2 between Pt surfaces when $H \perp k$ (a) and $H \parallel k$ (b). Experimental points correspond to the following pressures (Knudsen numbers): \circ —0.39 Torr (0.08), \bullet —0.16 Torr (0.2), \blacktriangle —0.064 Torr (0.5), $+\text{---}$ —0.032 Torr (1), \times —0.016 Torr (2), \diamond —0.008 Torr (4), \square —0.004 Torr (8), Δ —0.002 Torr (16).

Figure 4 shows the experimental results for $(\Delta Q/Q)_{\text{sat}}^{\perp}$ and $(\Delta Q/Q)_{\text{sat}}^{\parallel}$ for oxygen as functions of pressure (Knudsen numbers) in the case of gold and platinum surfaces. It is clear that the quantities $(\Delta Q/Q)_{\text{sat}}^{\perp}$ and $(\Delta Q/Q)_{\text{sat}}^{\parallel}$ are independent of gas pressure and surface material for $Kn \ll 1$. They are determined exclusively by the nature of the interaction between the O_2 molecules, and are respectively equal to 0.0126 and 0.0083.^[6]

For pressures corresponding to $Kn > 8$, the quantities $(\Delta Q/Q)_{\text{sat}}^{\perp}$ and $(\Delta Q/Q)_{\text{sat}}^{\parallel}$ are also independent of the gas pressure, but are very dependent on the surface material. For TME in O_2 interacting with Au or Pt surfaces, the values of $(\Delta Q/Q)_{\text{sat}}$ are, respectively, $(1.5 \pm 0.1) \times 10^{-3}$ and $(1.1 \pm 0.1) \times 10^{-3}$. These are lower by an order of magnitude as compared with the analogous quantities for the Senftleben effect. They are determined by the nature of the inelastic interaction between O_2 and the gold or platinum surface. The value of $(\Delta Q/Q)_{\text{sat}}^{\parallel}$ in O_2 interacting with a platinum surface is lower by an order of magnitude than $(\Delta Q/Q)_{\text{sat}}^{\perp}$ whilst, for O_2 interacting with the gold surface, it is found that $(\Delta Q/Q)_{\text{sat}}^{\parallel} = 0$ to within experimental error.

Figure 4 shows that the ratio $(\Delta Q/Q)_{\text{sat}}^{\parallel} / (\Delta Q/Q)_{\text{sat}}^{\perp}$ for TME in O_2 interacting with a platinum surface is $(1.0 \pm 0.3) \times 10^{-1}$, whereas, for O_2 on a gold surface, this ratio is equal to zero. It is interesting to compare the ratio $(\Delta Q/Q)_{\text{sat}}^{\parallel} / (\Delta Q/Q)_{\text{sat}}^{\perp}$ for TME with the analogous quantity for the Senftleben effect in oxygen which, as can be seen from Fig. 4, is equal to 0.66. Figure 5 shows the change in the ratio $(\Delta Q/Q)_{\text{sat}}^{\parallel} / (\Delta Q/Q)_{\text{sat}}^{\perp}$ during

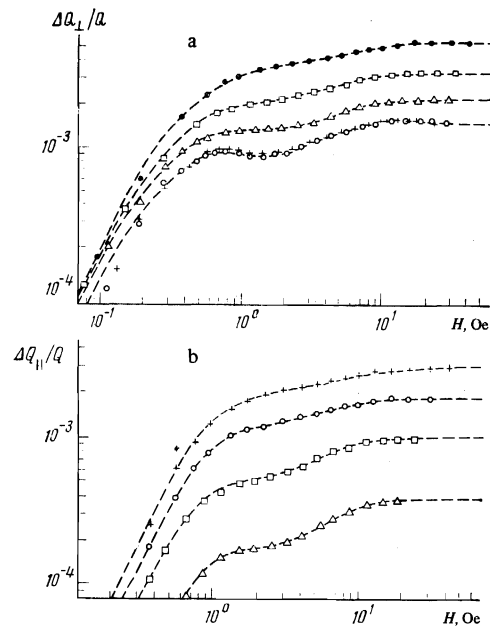


FIG. 3. Ratio $\Delta Q/Q$ as a function of H for O_2 between Au surfaces when $H \perp k$ (a): \bullet — $p=0.032$ Torr ($Kn \approx 1$), \square — $p=0.016$ Torr ($Kn \approx 2$), Δ — $p=0.008$ Torr ($Kn \approx 4$), \circ — $p=0.004$ Torr ($Kn \approx 8$), $+\text{---}$ — $p=0.0016$ Torr ($Kn \approx 20$); and when $H \parallel k$ (b): $+\text{---}$ — $p=0.046$ Torr ($Kn \approx 0.7$), \circ — $p=0.032$ Torr ($Kn \approx 1$), \square — $p=0.020$ Torr ($Kn \approx 1.6$), Δ — $p=0.013$ Torr ($Kn \approx 2.5$).

the transition from high pressures corresponding to the Senftleben effect to low pressures corresponding to the TME conditions. This difference between the Senftleben effect and TME suggests a difference in the polarizations of the angular momenta of the molecules resulting from the scattering of O_2 by O_2 and by a solid surface. We also note that the ratio $(\Delta Q/Q)_{\text{sat}}^{\parallel} / (\Delta Q/Q)_{\text{sat}}^{\perp}$ for the Senftleben effect is close to 2/3 for most diatomic gases, whereas the corresponding figure for TME depends both on the nature of the gas and of the surface. For example, for the nonparamagnetic diatomic gas N_2 interacting with Au surfaces, this ratio is close to $\frac{1}{2}$.^[5]

Figures 6–8 show that the ratios $(\Delta Q/Q)^{\perp}$ and $(\Delta Q/Q)^{\parallel}$ for TME in O_2 are independent of pressure, and each type of surface has its own universal dependence (for a fixed separation L between the hot and cold surfaces between which heat transfer takes place). The values of

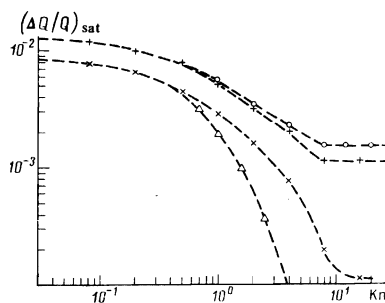


FIG. 4. Ratio $(\Delta Q/Q)_{\text{sat}}$ as a function of Kn . The experimental points correspond to the following conditions: \circ — $H \perp k$, Δ — $H \parallel k$ in O_2 -Au, and $+\text{---}$ — $H \perp k$, \times — $H \parallel k$ in O_2 -Pt.

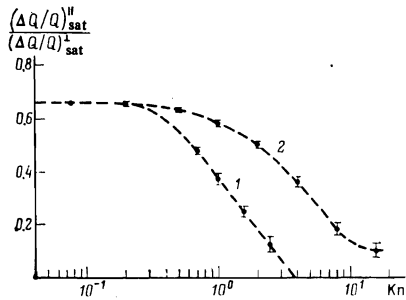


FIG. 5. Ratio $(\Delta Q/Q)_{\text{sat}}^{\text{II}} / (\Delta Q/Q)_{\text{sat}}^{\text{I}}$ as a function of Kn for O_2 -Au (1) and O_2 -Pt (2).

$(HL)_{\text{max}}$, determined from the position of the maxima and the values of $(\Delta Q/Q)_{\text{sat}}$ are shown in Table I.

The presence of the two maxima on $(\Delta Q/Q)^{\text{I}}$ and $(\Delta Q/Q)^{\text{II}}$ plotted as functions of H , is explained by the fact that there are three magnetic modifications of O_2 molecules in oxygen, which differ from one another only by the magnetic moments. Thus, in statistical equilibrium, one-third of the molecules has magnetic moments μ parallel to the orbital angular momentum \mathbf{M} and given by $\mu \approx -2\mu_0 \mathbf{M}/M$ for $\sigma = +1$ [σ is the component of the electron spin s ($s=1$) along the direction of the total angular momentum and μ_0 is the Bohr magneton], one-third of the molecules has $\mu \approx +2\mu_0 \mathbf{M}/M$ for $\sigma = -1$, and the remaining third has $\mu \approx -2\mu_0 \hbar \mathbf{M}/M^2$ for $\sigma = 0$. It follows that TME in oxygen can be looked upon as the sum of two effects involving O_2 molecules with $\sigma = \pm 1$ and $\sigma = 0$ (since the effect is even in the field), the first of which is observed in fields that are smaller by a factor of \bar{J} than those corresponding to the second (\bar{J} is the mean rotational quantum number). Comparison of the values of H_{max} for $\sigma = \pm 1$ and $\sigma = 0$ shows that, for oxygen in the temperature range 300–400 °K, the mean quantum number is $\bar{J} \approx 20$, whereas the formula $\bar{J} \approx \sqrt{2IkT}/h$ yields $\bar{J} = 12$ –14. Hence, it follows that the main contribution to TME is provided by rapidly rotating molecules with perturbed high rotational states, i. e., the rotational quantum number J is greater than the most probable value \bar{J} . We note that the considerable contribution of rapidly rotating molecules to the Scott effect (rotation of a heated cylinder in a molecular gas in the presence of a magnetic field parallel to the axis of the cylinder) was

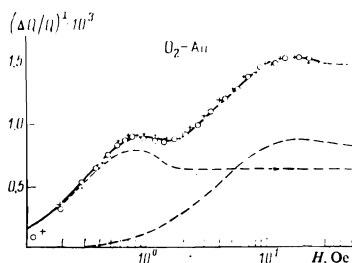


FIG. 6. Ratio $(\Delta Q/Q)^{\text{I}}$ as a function of H for O_2 -Au. The experimental points correspond to the following pressures: \circ —0.004 Torr ($\text{Kn} \approx 8$), $+$ —0.0016 Torr ($\text{Kn} \approx 20$). Solid line—theoretical dependence calculated from (5.4). Broken curve shows the individual contributions of O_2 molecules with $\sigma = \pm 1$ and $\sigma = 0$ to the ratio $(\Delta Q/Q)^{\text{I}}$.

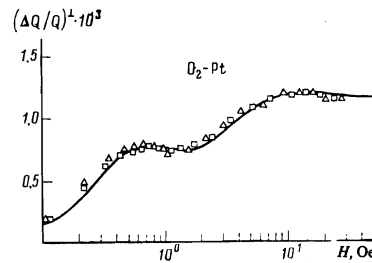


FIG. 7. Ratio $(\Delta Q/Q)^{\text{I}}$ as a function of H for O_2 on Pt. The experimental points correspond to the following pressures: \square —0.004 Torr ($\text{Kn} \approx 8$), \triangle —0.002 Torr ($\text{Kn} \approx 16$). Solid curve— theoretical dependence calculated from (5.9).

pointed out in^[10].

According to the foregoing discussion, the quantity $(\Delta Q/Q)_{\text{sat}}$ in oxygen is equal to the sum of $(\Delta Q/Q)_{\text{sat}}^{\sigma=\pm 1}$ and $(\Delta Q/Q)_{\text{sat}}^{\sigma=0}$ and, since in the free-molecular state $\Delta Q_{\text{sat}} \propto n_{\sigma}$, $Q \propto n$ (n_{σ} is the number of O_2 molecules per unit volume with given value of σ , and $n = \sum_{\sigma} n_{\sigma}$), it follows from the above experimental results that the interaction of O_2 molecules with Au and Pt surfaces leads to the non-equilibrium population of the states of the oxygen molecules with different values of σ . This follows from an analysis of the curves in Figs. 2 and 3 in relation to the change in the ratio of $(\Delta Q/Q)_{\text{sat}}$ for O_2 molecules with $\sigma = \pm 1$ and $\sigma = 0$ in the course of transition to lower pressures, for which the interaction between O_2 and the surface becomes appreciable.

Comparison of $(\Delta Q/Q)_{\text{sat}}^{\sigma=\pm 1}$ and $(\Delta Q/Q)_{\text{sat}}^{\sigma=0}$ for O_2 -Au and O_2 -Pt shows that the number of O_2 molecules with $\sigma = 0$ is greater than the corresponding equilibrium value. The estimates given in Sec. 5, based on a comparison between experimental and theoretical curves, show that this number is $\sim 56\%$ for O_2 -Au and $\sim 50\%$ for O_2 -Pt (as a fraction of the total number of molecules). We note that the appearance of nonequilibrium population of O_2 states with different values of σ was previously observed^[6] in the course of studies of the Senftleben effect at low pressures. The estimates given in^[6] are $(n_{\sigma=0}/n) \approx 0.29$ for $\text{Kn} \ll 1$ (which is close to the equilibrium value of $1/3$) and $(n_{\sigma=0}/n) \gtrsim 0.56$ for $\text{Kn} \gtrsim 1$ (when one of the surfaces is gold and the other glass).

4. THEORY OF TME IN OXYGEN

In contrast to nonparamagnetic gases,^[5] TME in oxygen requires special theoretical description. Molecular oxygen is in the $^3\Sigma$ electronic ground state, and has an uncompensated resultant electron spin $s=1$ and zero electronic orbital angular momentum (Hund's case b).

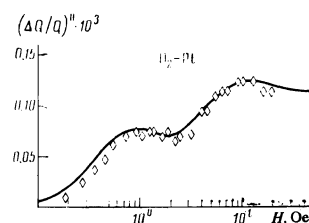


FIG. 8. Ratio $(\Delta Q/Q)^{\text{II}}$ as a function of H for O_2 on Pt when $\text{Kn} \approx 16$. Solid curve shows the theoretical dependence calculated from (5.8).

TABLE I.

Gas-solid combination	Field direction	$(HL)_{\max}, \text{Oe mm}$		$\left(\frac{\Delta Q}{Q}\right)_{\text{sat}}$
		$\sigma = \pm 1$	$\sigma = 0$	
O ₂ -Au	H ⊥ k	1.5 ± 0.1	27 ± 2	$(1.5 \pm 0.1) \cdot 10^{-8}$ 0
	H k	-	-	
O ₂ -Pt	H ⊥ k	1.2 ± 0.1	23 ± 2	$(1.1 \pm 0.1) \cdot 10^{-2}$ $(1.1 \pm 0.2) \cdot 10^{-4}$
	H k	1.7 ± 0.1	20 ± 2	

The effective magnetic moment of oxygen due to the uncompensated electron spin is given by^[11]

$$\mu_{\text{eff}} = \gamma_{\sigma} M, \quad \gamma_{\sigma} = -\frac{2\mu_0}{M} \left[\sigma + \frac{\hbar}{M} \left(1 - \frac{1}{2} \sigma^2 \right) \right]. \quad (4.1)$$

It follows from (4.1) that the precession frequency $\omega_{\sigma} = \gamma_{\sigma} H$ of O₂ molecules in the magnetic field H depends on the orbital angular momentum M and the component σ of the spin along the direction of the total angular momentum.

To describe the effect, we must solve the kinetic equation

$$(v \nabla) f_{\sigma} + \gamma_{\sigma} [\mathbf{M} \times \mathbf{H}] \frac{\partial f_{\sigma}}{\partial \mathbf{M}} = 0 \quad (4.2)$$

subject to the boundary conditions for the distribution function $f_{\sigma}(\mathbf{v}, \mathbf{M})$ on the surfaces bounding the gas. According to^[3], the solution of (4.2) can be written in the form

$$f_{\sigma} = \sum_{lmk} \chi_{lm}(\mathbf{v}, M^2, \sigma) D_{mk}^{l*}(\theta_H, \varphi_H) Y_{lk}(\mathbf{M}) \exp\left(im \frac{\gamma_{\sigma} H z}{v_z} \right), \quad (4.3)$$

where $D_{mk}^l(\theta_H, \varphi_H)$ is the finite rotation matrix, θ_H and φ_H are the polar angles defining the directions of the magnetic field, and $Y_{lk}(\mathbf{M}) = M^l Y_{lk}(\theta_M, \varphi_M)$ is the spherical harmonic. The coordinate system is chosen so that the direction of the normal \mathbf{k} to one of the surfaces lies along the z axis. The functions χ_{lm} must be determined from the boundary conditions.

The general form of the boundary condition relating the distribution functions for the incident (f_{σ}^-) and reflected (f_{σ}^+) molecules has the form of an integral equation, the kernel of which is the probability density for the scattering of the molecules by the surface.^[12] For oxygen molecules, this can be written in the form

$$v_z f_{\sigma}^+(\mathbf{v}, \mathbf{M}) = \sum_{\sigma'} \int v_z' W(\mathbf{v}', \mathbf{M}', \sigma' \rightarrow \mathbf{v}, \mathbf{M}, \sigma; \mathbf{k}) f_{\sigma'}^-(\mathbf{v}', \mathbf{M}') d\mathbf{v}' d\mathbf{M}'. \quad (4.4)$$

The primes on $\mathbf{v}, \mathbf{M}, \sigma$ indicate that they refer to molecules incident on the surface. The scattering kernel W is a nonnegative normalized function satisfying the reciprocity relation (principle of detailed balancing).

Following^[5], we shall assume that the scattering probability can be written in the form

$$W = W_0 + \varepsilon W_1, \quad (4.5)$$

where W_1 is the nonspherical part of W and ε is a small parameter representing the departure from the spherical situation. The quantity W_0 describes elastic specular reflection and diffuse reflection which is isotropic in the orientation and direction of emission of the molecules. These processes are represented by the following scattering kernel:

$$W_0 = (1-\alpha) \delta(\mathbf{v}' - [\mathbf{v} - 2(\mathbf{k}\mathbf{v})\mathbf{k}]) \delta(\mathbf{M}' - \mathbf{M}) \delta(\sigma' - \sigma) + \alpha \frac{v_z \exp(-E/kT)}{\int v_z \exp(-E/kT) dv d\mathbf{M}}, \quad (4.6)$$

where α is the diffuse scattering coefficient, T is the surface temperature, and $E = mv^2/2 + M^2/2I$ is the energy of the molecule.

Substituting (4.5)–(4.6) into the integral equation (4.4), we obtain a system of boundary conditions relating the distribution functions for the incident and reflected molecules on both surfaces. Since the currents of incident and reflected molecules must be equal, this set of equations can be reduced to the form^[1]

$$\begin{aligned} f_{\sigma}^+(\mathbf{v}, \mathbf{M}) &= (1-\alpha) f_{\sigma}^-(\mathbf{v} - 2(\mathbf{k}\mathbf{v})\mathbf{k}, \mathbf{M}) + \alpha n \frac{\sqrt{T_2}}{\sqrt{T_2} + \sqrt{T_1}} f(T_1) \\ &+ \varepsilon \frac{\sqrt{T_2}}{\sqrt{T_2} + \sqrt{T_1}} f(T_1) [G(f^-) + G(f^+)] + \varepsilon \sum_{\sigma'} \int \frac{v_z'}{v_z} W_1 f_{\sigma'}^-(\mathbf{v}', \mathbf{M}') d\mathbf{v}' d\mathbf{M}', \\ f_{\sigma}^-(\mathbf{v}, \mathbf{M}) &= (1-\alpha) f_{\sigma}^+(\mathbf{v} - 2(\mathbf{k}\mathbf{v})\mathbf{k}, \mathbf{M}) + \alpha n \frac{\sqrt{T_1}}{\sqrt{T_2} + \sqrt{T_1}} f(T_2) \\ &+ \varepsilon \frac{\sqrt{T_1}}{\sqrt{T_2} + \sqrt{T_1}} f(T_2) [G(f^+) + G(f^-)] + \varepsilon \sum_{\sigma'} \int \frac{v_z'}{v_z} W_1 f_{\sigma'}^+(\mathbf{v}', \mathbf{M}') d\mathbf{v}' d\mathbf{M}'. \end{aligned} \quad (4.7)$$

In these expressions, n is the number density of the gas particles, T_1 and T_2 are the temperatures of the surfaces bounding the gas, and

$$\begin{aligned} f(T) &= \left(\frac{m}{2\pi kT} \right)^{3/2} \frac{1}{IkT} \exp\left(-\frac{E}{kT} \right), \\ G(f^{\pm}) &= \sum_{\sigma'} \int \frac{v_z'}{v_z} W_1 f_{\sigma'}^{\pm}(\mathbf{v}', \mathbf{M}') d\mathbf{v}' d\mathbf{M}' dv d\mathbf{M}. \end{aligned}$$

The expression for the heat flux in a magnetic field can be obtained by using an expansion of the nonspherical part of the scattering probability W_1 in terms of spherical harmonic functions of the vectors $\mathbf{v}', \mathbf{M}', \mathbf{v}, \mathbf{M}, \mathbf{k}$. Since W_1 is a scalar, this expansion can be written in the form

$$\begin{aligned} W_1 &= v_z \exp\left(-\frac{E}{kT} \right) \sum_{\mu} \beta_{\mu}(v'^2, M'^2, \sigma', v^2, M^2, \sigma) A_{\mu}, \\ A_{\mu} &= \sum_n \begin{pmatrix} j_1 & j_2 & l_3 \\ m & -m & 0 \end{pmatrix} Y_{l_3 0}(\mathbf{k}) \sum_{m_1, m_2} \langle l_1' m_1' l_2 m_2 | j_1 m \rangle Y_{l_1' m_1'}(\mathbf{v}') \\ &\times Y_{l_2 m_2}(\mathbf{v}) \sum_{m_3} \langle l_2' m_2' l_3 m_3 | j_2 -m \rangle Y_{l_2' m_2'}(\mathbf{M}') Y_{l_3 m_3}(\mathbf{M}), \\ \mu &= \{(l_1' l_1) j_1, (l_2' l_2) j_2, l_3\}. \end{aligned} \quad (4.8)$$

In these expressions, $\langle \dots | \dots \rangle$ is the Clebsch–Gordan coefficient and $(:::)$ is the Wigner $3j$ symbol. The requirement of normalization and reciprocity introduces a number of restrictions on the possible terms in the expansion of W_1 . Thus, it is readily shown that nonzero contributions to the effect are provided by terms in the expansion (4.8) with

$$l_2'=0 \text{ and } l_2 \neq 0 \quad (\text{or } l_2' \neq 0 \text{ and } l_2=0). \quad (4.9)$$

The dependence of the nonspherical part of the scattering probability W_1 on σ' and σ is taken into account in the coefficient β_μ , which we shall give in the form of an expansion in terms of the orthogonal functions $\varphi_n(\sigma)$:

$$\beta_\mu = \sum_{n',n} \alpha_{n',n}(v'^2, M'^2, v^2, M^2) \varphi_{n'}(\sigma') \varphi_n(\sigma). \quad (4.10)$$

According to [11], the first three functions $\varphi_n(\sigma)$ can be written in the form

$$\varphi_0=1, \quad \varphi_1=\sqrt{2}\sigma, \quad \varphi_2=\sqrt{7/2}(\sigma^2-\sigma^2). \quad (4.11)$$

Since the observed change in the heat flux in a magnetic field is an even function of the magnetic field, i.e., it is independent of the sign of γ_σ and, consequently of the sign of σ , we need only retain even terms in σ' and σ in (4.10) (to describe the experimental data, it is sufficient to confine our attention to φ_0 and φ_2).

The dependence of the coefficients $\alpha_{n',n}$ on v'^2 , M'^2 , v^2 , M^2 can be written as an expansion in terms of the orthonormal Sonine polynomials:

$$\alpha_{n',n} = \sum_{r',r} a_{n',n}^{pqr} S_{r'}(v'^2) S_r(M'^2) S_{r'}(v^2) S_r(M^2). \quad (4.12)$$

It is readily shown (using the normalization conditions for the function and the orthogonality of the Sonine polynomials) that the expansion given by (4.12) is, at the same time, subject to the following restrictions:

$$r' = \frac{l_1'+2}{2}, \quad s' = \frac{l_2'}{2} = 0, \quad p, q \neq 0. \quad (4.13)$$

When the heat flux is calculated in the second approximation in ε , it is found that nonzero contributions to the flux are provided only by terms with $p=0$, $q=1$ and $p=1$, $q=0$ in (4.12). It will be shown below that the orders r and s of the Sonine polynomials written as functions of v^2 and M^2 are given by the orthogonality of the polynomials when the heat flux is calculated in the second approximation in ε in the absence of the field, and are given by

$$r=l_1+1, \quad s=l_2. \quad (4.14)$$

The heat flux in the gas between two parallel surfaces is given by

$$Q = \int v_x E [f_{\sigma^+}(v, M) - f_{\sigma^-}(v-2(kv)k, M)] dv dM. \quad (4.15)$$

The problem of the heat flux in a magnetic field can be solved with the aid of perturbation theory. In the zero-order approximation in ε , we have

$$Q_0 = \frac{3}{2} \frac{\alpha}{2-\alpha} \sqrt{\frac{2k}{\pi m}} nk (T_1 T_2 - T_2 T_1). \quad (4.16)$$

The function $Q(H)$ appears only in the second approximation in ε . Proceeding by analogy with (5), we can show that the change in the heat flux for $\mathbf{H} \parallel \mathbf{k}$ and $\mathbf{H} \perp \mathbf{k}$ is, respectively,

$$[\Delta Q_{\parallel}(\omega\tau)]_{\mu\nu} = \sum_{\sigma} A^{\sigma} [J_0(\omega\sigma\tau) - J_{\nu}(\omega\sigma\tau)], \quad (4.17)$$

$$[\Delta Q_{\perp}(\omega\tau)]_{\mu\nu} = \sum_{\sigma} \left[B_{\nu}^{\sigma} J_0(\omega\sigma\tau) - \sum_{k=1}^{l_2} B_k^{\sigma} J_k(\omega\sigma\tau) \right]. \quad (4.18)$$

In these expressions, A^{σ} and B_k^{σ} ($k=0, 1, \dots, l_2$) are quantities which do not depend on the field and can readily be evaluated for each particular expansion of W_1 (4.8) with a definite set of indices $\mu = \{(l_1' l_1) j_1, (0 l_2) l_2, l_3\}$, and $\nu = |m_2|$. The integrals $J_k(\omega\sigma\tau)$ for $l_1' + l_1 + l_3 + m_2 = \text{even}$ and $l_1' + l_1 + l_3 = m_2 = \text{odd}$ have the following form, respectively:

$$J_k^{(1)} = \int_0^{\infty} g(x, y) \exp(-x^2 - y^2) \psi_k^{(1)}(x, y) dx dy, \quad (4.19)$$

$$J_k^{(2)} = \int_0^{\infty} g(x, y) \exp(-x^2 - y^2) \psi_k^{(2)}(x, y) dx dy, \quad (4.20)$$

where $x = v_x(m/2kT)^{1/2}$, $y = M(2IkT)^{-1/2}$. The functions $\psi_k^{(1)}$ and $\psi_k^{(2)}$ depend on the magnetic field H through the product $(\omega\sigma\tau)$, where $\omega\sigma = \gamma_\sigma H$ is the precession frequency, and $\tau = L/v_x$ is the characteristic time of flight of the molecules between the walls. They are given by

$$\psi_k^{(1)} = \frac{(1-\alpha)^2 + \alpha(2-\alpha) \cos(k\omega\sigma\tau) - (1-\alpha) \cos(2k\omega\sigma\tau)}{1-2(1-\alpha)^2 \cos(2k\omega\sigma\tau) + (1-\alpha)^4}, \quad (4.21)$$

$$\psi_k^{(2)} = \frac{(1-\alpha)^2 - \alpha(2-\alpha) \cos(k\omega\sigma\tau) - (1-\alpha) \cos(2k\omega\sigma\tau)}{1-2(1-\alpha)^2 \cos(2k\omega\sigma\tau) + (1-\alpha)^4}. \quad (4.22)$$

The field-independent functions $g(x, y)$ are polynomials in x and y of degree $2l_1 + 1 + 4t$ and $2l_2 + 1 + 4u$, respectively.

It is important to note that (4.17) and (4.18) differ from the expressions for $\Delta Q_{\parallel}(\omega\tau)$ and $\Delta Q_{\perp}(\omega\tau)$ for nonparamagnetic gases [5] by additional averaging over the orbital angular momenta of the molecules and σ .

5. COMPARISON OF THEORY WITH EXPERIMENT AND DETERMINATION OF SCATTERING PROBABILITY

Theoretical determination of experimental results with the aid of the theory put forward in Sec. 4 presupposes that an analysis of some model expressions for the nonspherical part of the scattering probability W_1 has been used to select particular theoretical functions, and that these have been compared with the experimental functions. Analysis of experimental results is best begun with the dependence of $(\Delta Q/Q)_{\parallel}$ on H , since the theoretical expression for ΔQ_{\parallel} is much simpler than that for ΔQ_{\perp} [see (4.17) and (4.18)].

The particular feature of TME in O_2 interacting with a gold surface is the absence of a change in the heat flux in a magnetic field $\mathbf{H} \parallel \mathbf{k}$, i.e., $\Delta Q_{\parallel} = 0$ (see Sec. 3). Theoretical analysis shows that $\Delta Q_{\parallel} = 0$ if, in the expansion for W_1 (4.8), we retain the terms $\beta_{\mu} A_{\mu}$ with

$$j_i = 0 \quad \text{or} \quad l_i = 0. \quad (5.1)$$

Moreover, it is necessary that

$$l_1' + l_1 + l_2 + l_3 = \text{even}, \quad (5.2)$$

for which the sign of ΔQ_{\perp} is negative, and this is in agreement with the observed reduction in the heat flux in $\mathbf{H} \parallel \mathbf{k}$.

TABLE II.

μ	$g(x, y)$ for $t, u=0$	$\psi_k(x, y)$	$J_k(\omega_0\tau)$
{(00) 0, (01) 1.1}	xy^3	$\psi_1^{(2)}$	Fig. 9a
{(10) 1, (01) 1.0}	xy^3	$\psi_1^{(2)}$	Fig. 9a
{(10) 1, (01) 1.2}	xy^3	$\psi_1^{(2)}$	Fig. 9a
{(11) 0, (01) 1.1}	x^2y^2	$\psi_1^{(2)}$	Fig. 9b
{(20) 2, (01) 1.1}	xy^3	$\psi_1^{(2)}$	Fig. 9a
{(00) 0, (02) 2.2}	xy^5	$\psi_2^{(1)}$	Fig. 9c
{(10) 1, (02) 2.1}	xy^5	$\psi_2^{(1)}$	Fig. 9c
{(11) 0, (02) 2.2}	x^2y^5	$\psi_2^{(1)}$	Fig. 9d
{(20) 2, (02) 2.0}	xy^5	$\psi_2^{(1)}$	Fig. 9c
{(20) 2, (02) 2.2}	xy^5	$\psi_2^{(1)}$	Fig. 9c

Table II shows the possible first terms in the expansion for W_1 which ensure that $\Delta Q_{||} = 0$ with l'_1, l_1, l_2, l_3 equal to 0, 1, 2). Figures 9a-d show plots of $J_k(\omega_0\tau)$ for $t, u=0$. Comparison of the theoretical functions given in Fig. 9 with the experimental function $\Delta Q_1(H)$ given in Fig. 6 shows that the best agreement insofar as the size and position of the maxima along the $\omega_0\tau = \gamma_0\sqrt{m/2kT}LH$ axis are concerned is provided by the curves in Fig. 9a (model of W_1 with $l_1=0$ and $l_2=1$). We note that, when the polynomials $g(x, y)$ with $t, u \neq 0$ are taken into account, this results in the appearance in the expression for $\Delta Q_1(\omega\tau)$ (4.18) of the integrals $J_k(\omega_0\tau)$ with higher powers of x and y , which do not describe the experimental function $\Delta Q_1(H)$.

Thus, the expression given by (4.8) for the nonspherical part of the scattering probability W_1 for O_2 molecules on Au surface can contain only terms $\beta_{\mu_1}A_{\mu_1}$ with

$$\mu_1 = \{(l'_1)0, (01)1, l_3\}, l'_1 + l_3 = \text{odd}, \quad (5.3)$$

where $\beta_{\mu_1} = \beta_{\mu_1}(v'^2, M'^2, \sigma', \sigma)$ [in (4.12), $p=0, 1; q=1, 0; t, u=0$].

For the models defined by (5.3), the expression for the relative change in the heat flux in the magnetic field parallel to the surface assumes the form

$$\frac{\Delta Q_{\perp}}{Q_0} = -\frac{\varepsilon^2 A^2}{\alpha(2-\alpha)} \int xy^3 \exp(-x^2-y^2) \left\{ 2 \left(1 - \frac{3}{2} \frac{a_{20}}{a_{00}} \right)^2 \times [\psi_1^{(2)}(\omega_{\pm 1}\tau) - \psi_0^{(2)}(0)] + \left(1 + 3 \frac{a_{20}}{a_{00}} \right)^2 [\psi_1^{(2)}(\omega_0\tau) - \psi_0^{(2)}(0)] \right\} dx dy. \quad (5.4)$$

In this expression, Q_0 is the heat flux in zero field (zero-order approximation in ε), A is a constant, $a_{00} = 2a_{00}^{10} + a_{00}^{01}$ and $a_{20} = 2a_{20}^{10} + a_{20}^{01}$. The dimensionless parameters $\omega_{\pm 1}$ and $\omega_0\tau$ are given by

$$\omega_{\pm 1}\tau = \frac{2\mu_0}{\hbar} [J(J+1)]^{-1/2} (m/2kT)^{1/2} HL \frac{1}{xy}, \quad (5.5)$$

$$\omega_0\tau = \frac{2\mu_0}{\hbar} [J(J+1)]^{-1} (m/2kT)^{1/2} HL \frac{1}{xy^2}.$$

The expression given by (5.4) is essentially the sum of two expressions. The first of these describes the change in the heat flux in oxygen, the molecules of which are in the state with $\sigma = \pm 1$, and the second corresponds to the state with $\sigma = 0$. We note that the contribution of each term depends on a_{00} and a_{20} which, in turn, determine the parts of the scattering probability which depend

and do not depend on σ , respectively. In particular, when the scattering probability is independent of σ ($a_{20} = 0$), the contribution of O_2 molecules with $\sigma = \pm 1$ to ΔQ is greater by a factor of two than for $\sigma = 0$, i. e., it corresponds to the equilibrium distribution of the molecules over states with different σ .

Comparison of the theoretical function (5.4) (see the curves in Fig. 9a) with the experimental function (Fig. 6) enables us to determine the values of \bar{J} , a_{20}/a_{00} , and εA in (5.4). The solid curve in Fig. 6 shows the theoretical function (5.4) with the following parameters: $\alpha = 0.85$, $\bar{J} = 23$, $a_{20}/a_{00} = \frac{1}{3}$, $\varepsilon A = 4 \times 10^{-2}$. The broken curves in Fig. 6 show the individual contributions to $\Delta Q_{\perp}/Q_0$ for O_2 molecules with $\sigma = \pm 1$ and $\sigma = 0$. As can be seen from the figure, the theoretical function (5.4) agrees with the experimental results to within experimental error.

For TME in O_2 interacting with a platinum surface, the characteristic feature is the presence of both terms in the change of the heat flux in a magnetic field, where $(\Delta Q/Q)_{\text{sat}}^{\perp} \approx 10^{-1} (\Delta Q/Q)_{\text{sat}}^{\parallel}$ (see Sec. 3). We also note that the functions $\Delta Q_1(H)$ for O_2 interacting with Pt and Au are similar (the relative maxima have the same size and their positions on the H axis differ by approximately 20%). It is therefore natural to suppose that the main term in the model expression (4.8) for the nonspherical part of the scattering probability W_1 for O_2 on Pt is a term of the form given by (5.3). To describe the observed change in the heat flux in a magnetic field $H \parallel k$, we must take the second term in W_1 into account, which

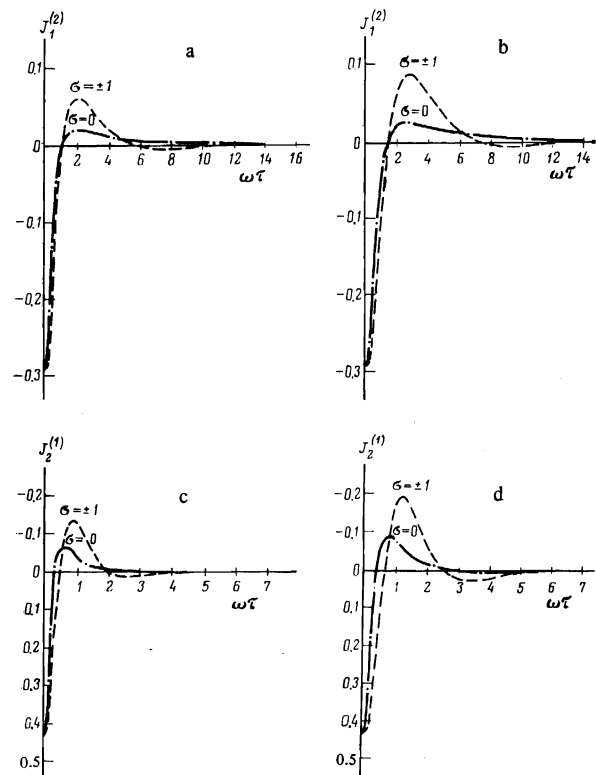


FIG. 9. The function $J_k(\omega_0\tau)$ for the model expressions for W_1 given in Table II.

gives both ΔQ_{\perp} and ΔQ_{\parallel} and is a small addition (~ 0.1) to the first term in (5.3).

Theoretical analysis similar to that performed for TME in O_2 interacting with a gold surface shows that the second term in W_1 when O_2 is scattered by a platinum surface can be the term

$$\mu_{\sigma} = \{ (l_1'1)l_1', (02)2, l_3, l_1'+l_2 = \text{odd}, l_1' \neq 0, \beta_{10} = \beta_{10}(v^2, M^2, \sigma', \sigma) \} \quad (5.6)$$

Thus, the model expression for the nonspherical part of the probability of scattering of O_2 molecules by Pt surfaces can be written in the form

$$W_1 = v_{\sigma} \exp(-E/kT) [\beta_{10}A_{10} + \beta_{11}A_{11}]. \quad (5.7)$$

Within the framework of this model, the expression for the change in the heat flux in magnetic fields respectively parallel and perpendicular to the normal to the surface can be written as follows:

$$\frac{\Delta Q_{\parallel}}{Q_0} = -\frac{\varepsilon^2 B^2}{\alpha(2-\alpha)} \int x^2 y^2 \exp(-x^2 - y^2) \sum_{\sigma} \Lambda_{\sigma} [\Psi_1^{(\sigma)}(\omega, \tau) - \Psi_0^{(\sigma)}(0)] dx dy. \quad (5.8)$$

$$\frac{\Delta Q_{\perp}}{Q_0} = -\frac{\varepsilon^2 C^2}{\alpha(2-\alpha)} \int x y^3 \exp(-x^2 - y^2) \sum_{\sigma} \Lambda_{\sigma} \left\{ [\Psi_1^{(\sigma)}(\omega, \tau) - \Psi_0^{(\sigma)}(0)] + \frac{B^2}{C^2} x^2 y^2 [\Psi_2^{(\sigma)}(\omega, \tau) + \Psi_1^{(\sigma)}(\omega, \tau) - \Psi_0^{(\sigma)}(0)] \right\} dx dy. \quad (5.9)$$

In these expressions, Λ_{σ} determines the contribution of O_2 molecules with a particular value of σ to the change in the heat flux. Thus, for $\sigma = \pm 1$

$$\Lambda_{\pm 1} = 2(1 - 3a_{20}/2a_{00})^2,$$

and for $\sigma = 0$

$$\Lambda_0 = (1 + 3a_{20}/a_{00})^2.$$

The quantities B and C are constants.

The solid curve in Figs. 7 and 8 shows the theoretical results calculated from (5.8) (see Fig. 8) and (5.9) (see Fig. 7) with $\alpha = 0.92$, $\bar{J} = 23$, $a_{20}/a_{00} = \frac{1}{12}$, $\varepsilon B = 0.8 \times 10^{-2}$, $\varepsilon C = 3.4 \times 10^{-2}$. As can be seen, the theoretical curves are in satisfactory agreement with experimental data. We note that, for the O_2 -Au and O_2 -Pt interactions, the contributions to the change in the heat flux by oxygen molecules with given σ are quite close to one another. For example, for $\sigma = 0$, we have $\Lambda_0/(\Lambda_0 + \Lambda_{\pm 1}) = 56$ and 50%, respectively.

It is interesting to compare the above model expressions for the nonspherical part of the scattering probability W_1 for O_2 molecules on Au and Pt, and the model expressions for W_1 for the nonparamagnetic gases N_2 , CO_2 , and CO interacting with Au.^[5] It turns out that when N_2 and CO_2 are scattered by Au the main terms in the expansion for W_1 in terms of the spherical harmonic functions of M are terms containing $Y_{2m}(M)$ whereas, for O_2 on Au, the probability W_1 contains only $Y_{10}(M)$. We also note that the model expression for W_1 in the case of CO also contains the term $Y_{10}(M)$. From the point of view of symmetry of the molecules, this result, i.e.,

the different angular dependence of W_1 on M , cannot be explained because the N_2 , CO_2 , and O_2 molecules have the same symmetry group ($D_{\infty h}$). It would appear that this difference in W_1 may be associated with the different nature of the interaction between the N_2 and CO_2 molecules, on the one hand, and O_2 and CO molecules, on the other, with the Au surface (it is well known that, in contrast to N_2 and CO_2 , the O_2 and CO molecules exhibit good chemisorption on Au). The reason for the small but appreciable difference between the model expressions for W_1 in the case of O_2 interacting with Au and Pt may be more fundamental and, in fact, connected with particular properties of the surface, for example, its catalytic activity.

In conclusion, let us consider the angular dependence of the distribution function for the molecules leaving the surface when the distribution function for the incident molecules is isotropic in the molecular orientation. Suppose that $f^- = f^-(\mathbf{v}', M'^2)$ so that, according to (4.7) and (5.3), we have for O_2 interacting with Au

$$f^+ = f_1^+(\mathbf{v}, M^2) + \varepsilon f_2^+(\mathbf{v}, M), \quad f_2^+ = F_1 \exp(-E/kT) \cos \theta_M, \quad (5.10)$$

where F_1 is the integral of f^- , which is independent of the orientation of the vectors \mathbf{v} and \mathbf{M} , and $f_1^+(\mathbf{v}, M^2)$ is the distribution function for the molecules reflected from the surface, which is isotropic in the orientation of \mathbf{M} . It follows from (5.10) that the probability of emission of a molecule with orbital angular momentum parallel and antiparallel to the normal of the surface (depending on the sign of F_1) is a maximum, and the axis of the molecule is then parallel to the surface. In the case of O_2 interacting with Pt, (5.7) shows that the anisotropic part of the distribution function for molecules reflected from the surface is augmented in (5.10) by the term

$$F_2 \exp(-E/kT) \sin \theta_v \sin \theta_M \cos \theta_M \cos(\varphi_M - \varphi_v), \quad (5.11)$$

where $|F_2| \sim 10^{-1} |F_1|$. Here again, the probability of emission of a molecule with the orientation in which the axis of the molecule is parallel to the surface is greater than the emission probability for a molecule with axis perpendicular to the surface. However, in contrast to O_2 on Au, in the scattering of O_2 by Pt, the probability of emission of a molecule depends on the direction of emission.

The authors are indebted to L. A. Maksimov for discussing the results of the present research and for useful advice, and to S. V. Sergeev for assistance in the preparation of the probes.

¹When the analogous boundary equation was derived in^[5], it was incorrectly assumed that $T_1 = T_2$. However, this does not affect the final expression obtained in^[5] for the heat flux in a magnetic field.

¹V. D. Borman, L. A. Maksimov, B. I. Nikolaev, and V. I. Troyan, Dokl. Akad. Nauk SSSR 207, 1082 (1972) [Sov. Phys. Dokl. 17, 1170 (1973)].

²V. D. Borman, V. S. Laz'ko, and B. I. Nikolaev, Zh. Eksp. Teor. Fiz. 63, 886 (1972); 66, 1343 (1974) [Sov. Phys. JETP

- 36, 466 (1972); 39, 657 (1974)].
- ³V. D. Borman, L. A. Maksimov, B. I. Nikolaev, and V. I. Troyan, *Zh. Eksp. Teor. Fiz.* 64, 526 (1973) [*Sov. Phys. JETP* 37, 269 (1973)].
- ⁴S. Yu. Krylov, V. D. Borman, B. I. Nikolaev, and V. I. Troyan, *Zh. Eksp. Teor. Fiz.* 67, 2122 (1974) [*Sov. Phys. JETP* 40, 1053 (1975)].
- ⁵V. D. Borman, B. I. Buttsev, S. Yu. Krylov, B. I. Nikolaev, and V. I. Troyan, *Zh. Eksp. Teor. Fiz.* 70, 929 (1976) [*Sov. Phys. JETP* 43, 484 (1976)].
- ⁶V. D. Borman, B. I. Nikolaev, and V. A. Ryabov, *Zh. Eksp. Teor. Fiz.* 67, 1377 (1974) [*Sov. Phys. JETP* 40, 684 (1975)].
- ⁷L. L. Gorelik, Yu. N. Redkobodoyi, and V. V. Spnitsyn, *Zh. Eksp. Teor. Fiz.* 48, 761 (1965) [*Sov. Phys. JETP* 21, 503 (1965)].
- ⁸L. J. F. Hermans, J. M. Koks, A. F. Hengeveld, and H. F. D. Knaap, *Physica* 50, 410 (1970).
- ⁹J. J. M. Beenakker and F. R. McCourt, *Ann. Rev. Phys. Chem.* 21, 47 (1970).
- ¹⁰G. G. Scott, G. W. Smith, and D. L. Fry, *Phys. Rev. A* 2, 2080 (1970).
- ¹¹L. A. Maksimov, *Zh. Eksp. Teor. Fiz.* 61, 604 (1971) [*Sov. Phys. JETP* 34, 322 (1971)].
- ¹²C. Cercignani, *Mathematical Methods in the Kinetic Theory of Gases*, Plenum Press, New York, 1969 (Russ. transl., Mir, M., 1972).

Translated by S. Chomet

Structure of a transverse shock wave in a plasma

A. L. Velikovich and M. A. Liberman

Institute of Physics Problems, USSR Academy of Sciences

(Submitted April 13, 1976)

Zh. Eksp. Teor. Fiz. 71, 1390-1411 (October 1976)

The structure of a shock wave front propagating in a fully ionized collision-dominated plasma perpendicular to the direction of the magnetic field is determined for arbitrary values of $\beta = 8\pi p/H^2$. It is shown that in the case of a magnetized plasma ($\Omega_e \tau_e > 1$) the wave front structure is determined by the ion viscosity and by the dispersion due to inertia of the electrons. The dispersion is more important at small values of β , and the structure of the wave front consists of oscillations that decay behind the wave front. At finite values of β the shock wave front is monotonic. In a shock wave with a sufficiently big temperature discontinuity, however, dispersion predominates at the beginning of the front and leads to the appearance of decaying oscillations ahead of the shock wave front. The Alfvén Mach numbers that are critical for the effect of dispersion are found. Dispersion due to electron inertia is not essential in the case of an unmagnetized plasma ($\Omega_e \tau_e < 1$). The width of the shock wave front is determined by Joule dissipation. The values of the critical Mach number ($M_a^h(\beta)$) above which Joule dissipation is insufficient for a continuous transition from a state ahead of the shock wave front to a state behind it are found. An isomagnetic discontinuity is produced behind the shock wave front in this case. The structure of the isomagnetic discontinuity, which is determined by the electron thermal conductivity, ion viscosity, and ion thermal conductivity, is found.

PACS numbers: 52.35.Lv

The structure of transverse shock waves in a plasma has been the subject of many theoretical as well as experimental studies (see, e.g., the review^[1] and the book^[2]). In view of the great variety of interactions of particles in the plasma, the structure of the shock wave is determined by various dissipative processes or dispersion effects, depending on the magnetic field strength and on the relations between the plasma parameters.

The first studies of shock waves in plasma^[3,4] yielded only a qualitative picture of the structure of the shock-wave front in the limit of a strong shock wave and under the assumption that the wavefront is the result of ion viscosity. The authors of subsequent papers devoted to the structure of the front of collision shock waves limited themselves either to numerical calculations or arbitrarily left in the equations a dissipation of some sort, neglecting the dispersion and the remaining dissipative terms.^[5-9] Naturally, the region of applicability of the results obtained in this manner is not clear.

A number of studies^[10-12] yielded the values of the critical Mach numbers which specify the boundary above

which there exists no integral curve joining the states ahead and behind the shock-wave front.

In the present paper, the critical Mach numbers are obtained for arbitrary values of β . It is shown that the boundary shock-wave intensities defined by these numbers signify either that at high intensity the chosen principal dissipation is insufficient for the formation of the shock front, or that oscillations appear on the front as a result of predominance of dispersion at an intensity below the given value.^[13,14]

The magnetic field in the plasma is usually characterized by the ratio $\beta = 8\pi p/H^2$ of the gas pressure to the magnetic-field pressure. Collisionless shock waves correspond to the cold-plasma limit, i.e., $\beta \ll 1$. A more convenient parameter when using the structure of shock waves is the degree of plasma magnetization $\Omega_e \tau_e$, where $\Omega_{e,i} = eH/m_{e,i}c$ is the cyclotron (electron) frequency and

$$\tau_{e,i} = 3m_{e,i}^{1/2} T_{e,i}^{3/2} / 4\pi^{1/2} n_e e^2 \eta$$

is the corresponding time of the Coulomb collisions. It